Vehicle Dynamics Control Using Model Predictive Control Allocation Combined with an Adaptive Parameter Estimator

Chatrath, Karan; Zheng, Yanggu; Shyrokau, B.

DOI
10.4271/12-03-02-0009

Publication date
2020

Document Version
Final published version

Published in
SAE International Journal of Connected and Automated Vehicles

ARTICLE INFO
Article ID: 12-03-02-0009

doi:10.4271/12-03-02-0009

Vehicle Dynamics Control Using Model Predictive Control Allocation Combined with an Adaptive Parameter Estimator

Karan Chatrath,[1] Yanggu Zheng,[1] and Barys Shyrokau[1]

[1]Technische Universiteit Delft, The Netherlands

Abstract

Advanced passenger vehicles are complex dynamic systems that are equipped with several actuators, possibly including differential braking, active steering, and semi-active or active suspensions. The simultaneous use of several actuators for integrated vehicle motion control has been a topic of great interest in literature. To facilitate this, a technique known as control allocation (CA) has been employed. CA is a technique that enables the coordination of various actuators of a system. One of the main challenges in the study of CA has been the representation of actuator dynamics in the optimal CA problem (OCAP). Using model predictive control allocation (MPCA), this problem has been addressed. Furthermore, the actual dynamics of actuators may vary over the lifespan of the system due to factors such as wear, lack of maintenance, etc. Therefore, it is further required to compensate for any mismatches between the actual actuator parameters and those used in the OCAP. This is done by combining the MPCA solver with an online adaptive parameter estimation (APE) algorithm. In this study, an advanced solution to the OCAP is proposed by combining MPCA with APE. This solution coordinates differential braking and active front steering (AFS) of a passenger vehicle, to stabilize the lateral and yaw motion. The simulation results indicate that the APE+MPCA combination effectively accounts for actuator dynamics and actuator parameter mismatches.

History

Received: 30 Dec 2019
Revised: 13 Mar 2020
Accepted: 18 Jun 2020
e-Available: 08 Jul 2020

Keywords

Vehicle dynamics control, Control allocation, Model predictive control allocation, Adaptive parameter estimator, Vehicle stability

Citation

Chatrath, K., Zheng, Y., and Shyrokau, B., "Vehicle Dynamics Control Using Model Predictive Control Allocation Combined with an Adaptive Parameter Estimator," *SAE Int. J. of CAV* 3(2):2020, doi:10.4271/12-03-02-0009.

ISSN: 2574-0741
e-ISSN: 2574-075X

Introduction

The development of active safety systems and their wide application in road vehicles has resulted in a decrease in the number of accidents and fatalities. However, the need for further reducing the occurrence of accidents still exists. As a result, the continuous advancement of the state-of-the-art of active safety applications becomes necessary.

Differential braking has been used in active safety systems like electronic stability control (ESC) and is widely studied in literature. It aims to prevent the vehicle from spinning or drifting out of control especially when operated near its limits of handling. By applying individual wheel braking, the system generates a corrective yaw moment to stabilize vehicle motion. A detailed description of ESC systems is provided in [1]. Figure 1 generally shows that the purpose of the ESC systems is to prevent loss of vehicle lateral stability.

Further enhancement of safety can be achieved by equipping a road vehicle with additional actuators. The use of active suspensions to enhance vehicle roll stability and the application of active steering that allows the direct generation of lateral forces on the front axle are some examples of this. The coordination of multiple actuators for vehicle control falls in the domain of integrated vehicle motion control. Another reason for equipping a vehicle with multiple actuators is the introduction of redundancy. Redundancy in a system can enhance its overall reliability and guarantees safety even in the event of actuator failure.

In addition, an actuator equipped in a vehicle is capable of influencing more than one state of vehicle motion. This coupling between actuator commands and vehicle states presents an opportunity as well as a challenge. The opportunity lies in the use of one actuator for multiple degrees-of-freedom (DOF) motion control. On the contrary, the challenge presents itself in the form of nonlinear coupling between states of the system and actuator commands. This can result in undesirable system responses. An example of such behavior can be seen in ESC systems. With the use of differential braking, there is an inevitable and undesired decrease in the longitudinal velocity of the vehicle. The ability of a single actuator to influence multiple states warrants the use of a strategy that ensures effective coordination between actuator commands, to achieve the desired motion.

For vehicle stability control systems, in order to stabilize lateral and yaw vehicle motion, it is possible to combine differential braking with active front steering (AFS), resulting in integrated vehicle control. This combination of five actuators is used to control a single-vehicle state, i.e., yaw rate. The number of actuators outnumbering the states to be controlled is what qualifies a system as overactuated.

Actuators of a dynamic system are governed by their own dynamics. However, they are often neglected in control design for the sake of simplicity or under the assumption that actuators respond very quickly to a command. In general, if a dynamic system has n states to be controlled with m number of actuators available for control, and if the actuators outnumber the states, then

$$m > n \qquad \text{Eq. (1)}$$

When Equation 1 is satisfied, it may so happen that different combinations of multiple actuator commands may yield the same system response, making the system overactuated. This will be elaborated upon in the following section. The control of overactuated systems using all available actuators effectively is not trivial. The potential problems include nonlinear coupling between states and interference between actuator commands. To address these challenges, a strategy known as control allocation (CA) can be used. CA is suitable for integrated vehicle motion control applications. In addition, one of the key reasons for the popularity of integrated vehicle control in literature is that the vehicle motion can be controlled more precisely, thus achieving several control objectives by using several actuators.

In this study, a strategy is proposed in order to effectively coordinate multiple actuators using CA, while ensuring that the method accounts for actuator dynamics, as well as their position and rate limits. Even if actuator dynamics are considered, its exact parameters may be unknown or may vary during the operational cycle. This incomplete knowledge of actuator dynamics parameters is compensated by combining the rest of the control system with an online adaptive parameter estimator. The application focuses on differential braking combined with AFS for vehicle yaw rate control.

The main contribution of the study is the combination of model predictive CA and online adaptive parameter estimation (APE), which is capable of optimally coordinating multiple actuators and is robust against parameter uncertainties in the actuator dynamics.

FIGURE 1 Objective of ESC systems.

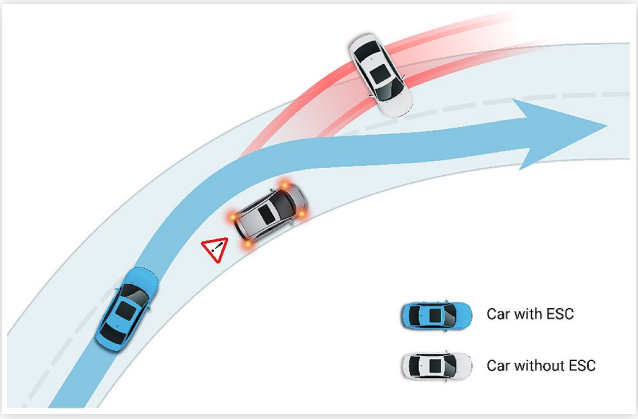

Adapted from Ref. [1]

Introduction to Control Allocation

CA is a technique to improve control of overactuated systems. The main function of a control allocator is the effective coordination of actuators. With CA, it becomes possible to divide the control system into sub tasks. A high-level controller computes a set of forces and moments required to regulate the response of the dynamic system. These high-level commands are also known as virtual control inputs, denoted by v, and are then fed into the control allocator, which in turn distributes them among the available actuators. The actuator commands are denoted by u. A general schematic is illustrated in Figure 2.

The CA technique has certain advantages. First, as the control system is separated into two tasks, the high-level control system is independent of any actuator configurations. This introduces modularity in the control system. The CA algorithm also tries to ensure that all actuators are utilized in the best way possible. To solve the CA problem, it is essential to have the knowledge of the relation between the virtual control input vector v and the actuator commands u (Figure 2). The virtual control inputs are high-level commands generated for each state to be controlled. Typically, a linearized mapping of the following form is derived:

$$v = Bu \qquad \text{Eq. (2)}$$

Here $v \in \mathbb{R}^n$ and $u \in \mathbb{R}^m$, and $m > n$. The matrix $B \in \mathbb{R}^{n \times m}$ is known as the control effectiveness matrix and is assumed to have full row rank. In other words, there may exists a set of actuator commands in the null-space of B which does not affect the virtual control input vector v. The system is in this sense considered overactuated.

The goal of the CA technique is to compute the vector u. Equation 2 is an underdetermined set of linear equations that may have a unique solution, may have infinite solutions, or may have no solution at all. The CA algorithm is designed in the way that it either finds this unique solution or the "best" among the infinite solutions. Or a vector u such that Bu is as close as possible to v, in some sense, in the event where there is no solution to the set.

In addition to solving the above set of underdetermined equations, the goal of the CA method is to ensure that actuators do not violate their constraints. More primitive CA methods had the objective of ensuring that actuator commands must lie within its range of operation [2]. Consequently, the solutions to Equation 2 were not necessarily "good solutions" to the CA problem. The CA problem was studied quite extensively in the 1990s for the purpose of aerospace applications. A geometrical interpretation to the CA problem is provided in [3]. The subject of optimization-based CA came to focus, when Bodson, in 2002, formulated a linear programming-based CA method known as "Direct Control Allocation" [4]. This progress inspired many researchers to focus on optimization-based CA. The following section provides a brief review of literature relevant to CA used for integrated vehicle motion control.

Control Allocation for Integrated Vehicle Motion Control

The review of CA methods, such as direct, pseudoinverse, daisy-chain, optimization-based and other, are well described theoretically in [2]. In the area of integrated control of vehicle dynamics, some of them have a wide application.

Pseudo-inverse CA based on Moore-Penrose inversion is an effective technique from the point of view of computational cost because this method requires only algebraic computation. The example of the application of this method is given in [5]. The yaw rate control by high-level proportional controller and coordination between friction brake system, front steering, and slip differential at the rear axle for a medium-sized luxury sports car is considered. Another example is the flatness-based high-level controller of vehicle velocity, vehicle sideslip angle, and yaw rate in [6]. Control demand is allocated between single-wheel steering, brake, drive, and suspension subsystems. The same type of allocation is used: in [7] yaw rate control with coordination between individually driven electric motors; in [8] the force allocation and coordination between steer-by-wire and individual-wheel electric powertrain; and in [9] the coordination between steer-by-and brake-by-wire systems in the case of actuator failure.

However, the major concern of classical pseudo-inverse CA is the neglect of control constraints omitting the actuator

FIGURE 2 CA general strategy.

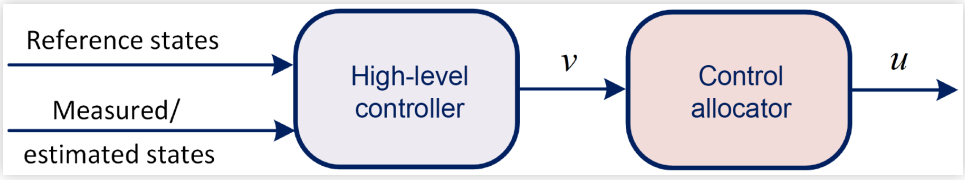

dynamics, tire friction limits, etc. An example of the method extension is the saturation and coordination of longitudinal/lateral forces by the pseudo-inverse CA with variable weightings [10].

Optimization-based CA with position, rate, and acceleration limits can effectively solve the constrained allocation problem. This kind of CA is mostly used in the literature. Only a few examples are considered below: in [11] the application of quadratic programming-based CA is proposed for different vehicle configurations including front/rear steering and individual torque control for each wheel. In [12] a control algorithm is developed based on the dynamic inversion of a nonlinear vehicle model and force allocation using nonlinear optimization with optimization constraints including adhesion potential utilization and limits of actuator dynamics. In [13] the controller of yaw rate and roll angle is developed using Lyapunov-based design for light commercial van and CA is based on weighted-norm constraints and a quadratic program. The allocation of generalized longitudinal and lateral forces and yaw torque between engine and brake torques is considered in [14]. The control law of the high-level controller is based on feedback linearization of a nonlinear vehicle model and proportional integral (PI) controller, which is extended with anti-windup based on back-calculation. To solve the optimization problem, the weighted least-squares (WLS) method with constraints including position and rate limits of actuators and force limits for each tire is implemented.

The optimization-based CA imposes high computation demand in real-time applications. To speed up it, the combination of various optimization solvers can be applied. For example, the hybrid optimization solver combining pseudo-inverse and fixed-point iteration methods is discussed in [15]. Another approach is the accelerated fixed-point method [16] with the termination of iterations, while solution distance exceeds allocation tolerance to improve convergence rate and reduce computational complexity. The hybrid steepest descent method for tire force allocation is proposed in [17] to reduce computational load. In this method, tire forces trend in the optimal direction, but their values are not necessarily optimal at each instant. The alternative approach for allocation between front/rear steer angles and additional yaw torque generated by in-wheel motors of an electric vehicle is discussed in [18]. The algorithm is based on infinity norm and the closed-form solution with piecewise linear functions and provides a low amount of operations. Another approach of optimization-based CA is the application of lexicographical optimization [19].

Instead of the application of optimization-based CA, which requires a solution at each instant, a dynamic CA method using dynamic update laws for control inputs is proposed in [20]. The dynamic CA shows higher computational efficiency compared to static one; however, its performance during maneuvers with high nonlinear behavior of vehicle and tires is lower compared to static one [21]. The researchers compare static allocation with nonlinear saturation constraints of tire forces solved by the interior-point method and dynamic allocation by Newton-like update law and Lagrange multipliers.

In general, the type of CA depends on actuator control inputs, desired cost functions, inverse tire model, number of active subsystems, and other factors. There are many examples of configurations of allocation parameters. One set of such parameters is longitudinal and lateral tire forces, e.g., [22]. For this set of parameters, only the problem of force allocation is addressed. Another set of parameters includes kinematic parameters based on tire inversion model where tire parameters can be obtained from force allocation [16]. Other parameters influencing tire behavior are steering angles, wheel speeds, and wheel load variations [6]. A third set of parameters includes reference control inputs of actuators such as brake pressure/torque, drive torque, and steering angle [14]. A parameter set may also comprise forces as well as actuator outputs, for instance, longitudinal forces and steering angle [9]; steering angles and yaw torque [18].

The key issues can be summarized as (i) the representation of actuator dynamics, (ii) the approximation of nonlinearities in the CA procedure, (iii) CA adaptation to uncertainties and disturbances, and (iv) the achievement of several objectives known as the multiobjective CA problem.

Although optimization-based methods consider actuator position and rate limits, actuator dynamics are still statically represented. Thereby, to handle actuator dynamics, some solutions have been proposed. One of them is the penalization of incremental step of control inputs taking into account previous behavior [23]. Another approach is the compensation of phase shift between desired and actual control effort [24]. The application of model predictive control allocation (MPCA) is also an option to account for actuator dynamics.

An MPCA approach for an overactuated electric vehicle is proposed in [25] for longitudinal and lateral control to allocate wheel torques taking in to account wheel slip and rate constraints. For brake blending applications, real-time MPCA is proposed in [26] using a linear actuator model. For critical driving situations, MPCA is proposed [27] for yaw stabilization to determine control inputs for four driving motors by commanding appropriate wheel slips. Also combination of MPCA with energy-efficient CA as an upper layer [28] or combination with classical WLS CA [29] are proposed. In addition to passenger electric vehicles, MPCA has been applied for an electric bike [30] and a heavy commercial vehicle [31]. The recent studies [32] have shown that in the case of different actuator dynamics and time delays, MPCA can be an effective solution to improve control performance.

In addition, when the desired demands have different frequencies, the frequency-apportioned CA [33] can separate control demand between high- and low-frequency components by a low-pass filter matrix.

One of the significant aspects of nonlinear CA is the approximation of tire forces and characteristics of an electric motor. The tire constraints can be obtained by piecewise linear approximation (rhombus) [17], friction ellipse concept [14], or more complex approximation techniques [34]. For the approximation of electric motor characteristics, the third- and fourth-order polynomials [35] can be applied. The losses of

an electric motor can be represented by the *second*-order polynomials [36].

Due to measurement noise, external disturbances, and the probability of actuator failure, a dynamic adaptive law of control effectiveness matrix to minimize uncertainties and to increase adaptability is proposed in [37]. One of the special issues of CA adaptability is its effectiveness in the case of the occurrence of actuator failures. The algorithms [38] of active fault diagnosis and control are proposed to maintain vehicle stability in the case of the fault of one electric motor using control gain estimation. The noniterative fault-tolerant control of electric motors based on off-line CA laws to maintain vehicle stability is proposed in [39]. In [9] the different scenarios of failures in the brake-by-wire system are considered to guarantee braking performance by the changing of the elements of the weighting matrix.

Concerning the multiobjective problem, the cost function of the CA problem typically covers two terms related to the minimization of allocation error and control actuation. Additional terms can be introduced into the CA cost function. The examples are as follows: (i) instantaneous power consumption of in-wheel motor in different modes [35], (ii) minimization of electric and mechanical losses of electric motor [36], and (iii) minimization of wheel slips [40]. In [41], a simplified cost function with the minimization of steering rate and the maximization of recuperation is formulated. Both the cost terms show similar results in overall energy consumption. In [42] the comparison of the following auxiliary cost terms, such as overall input motor power, the standard deviation of wheel slips, total longitudinal slip power loss, and the sum of the tire force coefficients, is carried out.

The results of CA investigation in the majority of research publications are limited by the simulation investigations in Simulink or in the software fusion of Simulink with commercial software, such as CarSim, IPG CarMaker, and veDyna. The investigation of CA for electrohydraulic brake system and axle electric motor using the real-time simulation via dSPACE 1006 and DS MicroAutoBox is discussed in [43]. The allocation between six vehicle subsystems is validated using a hardware-in-the-loop test rig with hardware components of the friction brake system and dynamic tire pressure system in real-time domain [44]. Optimization-based torque allocation is investigated using chassis dynamometer [45] to improve energy efficiency. The investigations of the longitudinal dynamics of an experimental electric ground vehicle with independently actuated in-wheel motors based on the method from [35] are proposed in [46]. The allocation of friction brake torques for lane-keeping assistance control of real test vehicle during double lane change is considered in [47].

From an industrial point of view, there are several patents related to the CA. The control system including CA and phase compensation of actuator commanded signal is patented by SAAB AB [48]. The solution has a general view and it covers CA for any vehicle subsystem. The real-time allocation of actuator torque by friction brakes and wheel motors is patented by GM [49]. The CA method is based on the least-squares formulation. It should be noted that in the patent the prioritization of vehicle subsystems using weighting matrices is mentioned without the detailed recommendations regarding the organization of prioritization. To summarize the literature survey, the following conclusions can be inferred:

- The integrated control typically involves two to four vehicle subsystems in the regulation process.
- Prevalent technique to distribute control demand for overactuated system is static optimization-based CA.
- Together with the minimization of allocation error and control efforts, the additional objectives, for example, related to energy characteristics can be introduced.
- Multiterm cost function can be formulated by the including additional terms or a penalization/prioritization of control inputs according to certain objectives.

Incorporation of actuator dynamics in the CA problem leads potentially to better performance. However, in the case of a significant mismatch between predefined model and real parameters, the adaptation is required. To address this issue, the following sections are dedicated to the formulation and application of the MPCA technique combined with online parameter estimation.

Model Predictive Control Allocation

MPCA is a CA technique based on model predictive control and it effectively accounts for the actuator dynamics. Model predictive control is an optimal control technique based on the idea of receding horizon control [50]. In the following description, a distinction is made between actuator commands and actuator response. The former is denoted by u_c while the latter is denoted by u.

Consider the following systems of actuators of an overactuated dynamic system. The number of actuators is considered to be N_u, and each actuator is modelled as a continuous-time, linear dynamical system. The dynamics of the ith actuator is of the form

$$\begin{aligned} \dot{x}_i(t) &= A_i x_i(t) + B_i u_{ci}(t-\delta_i) \\ u_i &= C_i x_i \end{aligned} \qquad \text{Eq. (3)}$$

where x_i represents the states of the ith actuator, u_{ci} represents the command sent to the ith actuator, and u_i is the response of the ith actuator. Here, $i \in (1, 2, 3, \ldots, N_u)$. As the MPCA algorithm operates in discrete time, each of these actuators can be discretized according to the zero-order hold (ZOH) operation. The resulting discrete-time dynamics of each actuator, without any loss of generality, can be represented as follows:

$$x_i(k+1) = A_{di}x_i(k) + B_{di}u_{ci}(k)$$
$$u_i(k) = C_{di}x_i(k) \quad \text{Eq. (4)}$$

The actuator dynamics can be combined into a single state-space description as such

$$\begin{bmatrix} x_1(k+1) \\ x_2(k+1) \\ \vdots \\ x_{N_u}(k+1) \end{bmatrix} = \begin{bmatrix} A_{d1} & 0 & \dots & 0 \\ 0 & A_{d2} & \dots & 0 \\ \vdots & \vdots & \ddots & 0 \\ 0 & 0 & \dots & A_{dN_u} \end{bmatrix} \begin{bmatrix} x_1(k) \\ x_2(k) \\ \vdots \\ x_{N_u}(k) \end{bmatrix} + \begin{bmatrix} B_{d1} & \dots & 0 \\ \vdots & \ddots & \vdots \\ 0 & \dots & B_{dN_u} \end{bmatrix} \begin{bmatrix} u_{c1}(k+1) \\ u_{c2}(k+1) \\ \vdots \\ u_{cN_u}(k+1) \end{bmatrix} \quad \text{Eq. (5)}$$

$$\begin{bmatrix} u_1(k) \\ u_2(k) \\ \vdots \\ u_{N_u}(k) \end{bmatrix} = \begin{bmatrix} C_{d1} & 0 & \dots & 0 \\ 0 & C_{d2} & \dots & 0 \\ \vdots & \vdots & \ddots & 0 \\ 0 & 0 & \dots & C_{dN_u} \end{bmatrix} \begin{bmatrix} x_1(k) \\ x_2(k) \\ \vdots \\ x_{N_u}(k) \end{bmatrix}$$

Equations 5 can be written in short as

$$x(k+1) = A_d x(k) + B_d u_c(k)$$
$$u(k) = C_{nd}x(k) \quad \text{Eq. (6)}$$

Equation 6 describes the combined discrete-time actuator dynamics. Recall that $v = Bu$. Using this, the following is obtained:

$$x(k+1) = A_d x(k) + B_d u_c(k)$$
$$u(k) = C_{nd}x(k)$$
$$BC_{nd} = C_d \quad \text{Eq. (7)}$$

Finally, the combined state-space representation of the actuator dynamics is

$$x(k+1) = A_d x(k) + B_d u_c(k)$$
$$v(k) = C_d x(k) \quad \text{Eq. (8)}$$

The sizes of each system matrix is as follows: $A_d \in \mathbb{R}^{N_s \times N_s}$, $B_d \in \mathbb{R}^{N_s \times N_u}$, $c_d \in \mathbb{R}^{N_o \times N_s}$. For formulating the MPCA problem, the notation shown above will be used consistently. To begin the formulation of the problem, three key pieces of information are necessary: the sampling time of the control system, the prediction horizon N_p, and the control horizon N_c.

Knowing this, Equation 8 can be iterated for future time steps as follows:

$$\begin{aligned} v(k+1) &= C_d A_d x(k) + C_d B_d u_c(k) \\ v(k+2) &= C_d A_d^2 x(k) + C_d A_d B_d u_c(k) \\ &\quad + C_d B_d u_c(k+1) \\ &\vdots \\ v(k+N_p) &= C_d A_d^{N_p} + C_d A_d^{N_p-1} B_d u_c(k) + \\ &\quad \cdots + C_d A_d^{N_p-N_c} B_d u_c(k+N_c-1) \end{aligned} \quad \text{Eq. (9)}$$

This set of iterated equations can be combined in a matrix form as such:

$$V(k) = Fx(k) + \phi U_c(k) \quad \text{Eq. (10)}$$

where

$$V(k) = \begin{bmatrix} v(k+1) \\ v(k+2) \\ \vdots \\ v(k+N_p) \end{bmatrix}$$
$$F = \begin{bmatrix} C_d A_d \\ C_d A_d^2 \\ \vdots \\ C_d A_d^{N_p} \end{bmatrix}$$
$$\phi = \begin{bmatrix} C_d B_d & \dots & 0_{N_o \times N_u} \\ C_d A_d B_d & \dots & 0_{N_o \times N_u} \\ \vdots & \dots & \vdots \\ C_d A_d^{N_p-1} B_d & \dots & C_d A_d^{N_p-N_c} B_d \end{bmatrix}$$
$$U_c = \begin{bmatrix} u_c(k) \\ u_c(k+1) \\ \vdots \\ u_c(k+N_c-1) \end{bmatrix} \quad \text{Eq. (11)}$$

Equation 10 is known as the predictor model based on which the controller operates. The matrix F is of a similar form as the observability matrix and the matrix ϕ is known as the Toeplitz matrix. The sizes of each of these matrices and vectors are $V(k) \in \mathbb{R}^{N_p N_o \times 1}$, $F \in \mathbb{R}^{N_p N_o \times N_s}$, $\phi \in \mathbb{R}^{N_p N_o \times N_u N_c}$, and $U_c(k) \in \mathbb{R}^{N_u \times N_c \times 1}$. The next step in the formulation of the MPCA problem is accounting for constraints imposed on the actuators. The position and rate constraints on actuators are formulated as per the work carried out in [23]:

$$u_{c,\mathrm{Min}} \le u_c(t) \le u_{c,\mathrm{Max}} \quad \text{Eq. (12)}$$

$$\rho_{c,\mathrm{Min}} \le \dot{u}_c(t) \le \rho_{c,\mathrm{Max}} \quad \text{Eq. (13)}$$

The rate limits can be rewritten as position limits by approximating the derivative as follows:

$$\dot{u}_c(t) \approx \frac{u_c(t) - u_c(t-T)}{T} \quad \text{Eq. (14)}$$

Based on this, the overall actuator constraints are

$$\underline{u_c} \;''\; u_c \;''\; \overline{u_c} \quad \text{Eq. (15)}$$

where

$$\begin{aligned} \underline{u_c} &= \max\left[u_{c,\mathrm{Min}}, u_c(t-T) + T\rho_{c,\mathrm{Min}}\right] \\ \overline{u_c} &= \min\left[u_{c,\mathrm{Max}}, u_c(t-T) + T\rho_{c,\mathrm{Max}}\right] \end{aligned} \quad \text{Eq. (16)}$$

The vector variable in the MPCA optimization problem is the vector U_c. The constraints need to be recast in terms of that. All the actuator commands computed through MPCA must satisfy all constraints throughout the control horizon N_c. This is done as such

$$\begin{aligned} A_{\mathrm{in}} &= \left[-I_{Nu\times N_c} \quad I_{Nu\times N_c}\right]^T \\ b_L &= \left[\underline{u_c} \quad \underline{u_c} \quad \dots \quad \underline{u_c}\right]^T \\ b_U &= \left[\overline{u_c} \quad \overline{u_c} \quad \dots \quad \overline{u_c}\right]^T \\ b_{\mathrm{in}} &= \left[-b_L \quad b_U\right]^T \end{aligned} \quad \text{Eq. (17)}$$

The relations in Equation 17 can be combined to yield a combined set of inequality constraints

$$A_{\mathrm{in}} U_c \le b_{\mathrm{in}} \quad \text{Eq. (18)}$$

The next step is to define the control allocator objective. Let us consider a high-level controller to be generating a virtual input vector or control demand namely v_{ref}. The control allocator must compute a set of actuator commands such that the actuators together produce this control demand throughout the prediction horizon. This can be captured by doing the following. The reference virtual control demand is defined referred to as V_{ref}:

$$V_{\mathrm{ref}} = \left[v_{\mathrm{ref}} \quad v_{\mathrm{ref}} \quad \dots \quad v_{\mathrm{ref}}\right]^T \quad \text{Eq. (19)}$$

where $V_{\mathrm{ref}} \in \mathbb{R}^{N_p N_o \times 1}$. Now, the MPCA optimization is formulated as such. It is formed such that it is a convex optimization problem. The cost function is defined as follows:

$$J = \left(V(k) - V_{\mathrm{ref}}\right)^T W \left(V(k) - V_{\mathrm{ref}}\right) + U_c(k)^T Q U_c(k) \quad \text{Eq. (20)}$$

The objective is to minimize the cost function J with respect to the vector U_c such that the constraints defined in Equation 18 are satisfied. Equation 10 is replaced in the cost function and expanded leading to the formation of a convex quadratic programming problem. The MPCA problem has several tuning parameters. There is the sample time of the control allocator T and the prediction and control horizons and the diagonal elements of the weighting matrices W and Q.

To solve this convex constrained quadratic programming problem, the following three methods were tested: the active set method, the Hildreth quadratic programming subroutine, and MATLAB's quadprog function which uses the interior point method. To compare the performance of each of these solvers, they were applied to solve the same problem. Moreover for each method the starting point (if applicable), the numerical tolerances and maximum number of iterations were set to the same values for an objective comparison. The result that this comparison yielded was that the Hildreth quadratic programming method showed the least amount of time taken per iteration and convergence in a fewer number of iterations compared to the active set method and the interior point method. Consequently, this QP solver was used for all simulations that were subsequently carried out.

Online Adaptive Parameter Estimation

The actuator dynamics described in the MPCA solver may deviate from the actual actuator dynamics. The above formulation of the MPCA problem is carried out under the assumption of linear actuator dynamics and accurate model parameters, which is not always feasible in practice. To address this, the MPCA algorithm is combined with an online adaptive parameter estimator. The outline of the method is presented below. Any actuator governed by linear dynamics can be rewritten without any loss on generality, in a linear-in-the-parameters parametric form as such:

$$z(k) = \phi_p^T(k)\theta(k) \quad \text{Eq. (21)}$$

where z and ϕ_p can be vectors that comprise filtered versions of the actuator input and output signals. The vector θ comprises all unknown parameters of the actuator to be estimated. Having framed the dynamics of the actuator in the above form, the auxiliary model-based recursive least-squares (AM-RLS) algorithm [51, 52] is used to estimate the elements of the vector θ in an adaptive manner.

The estimate of the parameter vector at the present time instant is referred to as $\hat{\theta}(k)$. Having explained the parametric model, the AM-RLS algorithm is presented as follows:

$$\hat{\theta}(k)=\hat{\theta}(k-1)+P(k)\phi_p(k)\left(z(k)-\phi_p^T(k)\hat{\theta}(k-1)\right)$$
$$P(k)=P(k-1)+\frac{P(k-1)\phi_p(k)\phi_p^T(k)P(k-1)}{1+\phi_p^T(k)P(k-1)\phi_p(k)} \quad \text{Eq. (22)}$$

The initial conditions ($P(1)$ and $\hat{\theta}(1)$) for the AM-RLS scheme is based on recommendations laid out in [51] and [52]. The AM-RLS algorithm operates under the following assumptions:

- Only the input and output of the system to be estimated are measured and all measurements are noise-free.
- The order of the system, number of zeros, and the input delay of the system are considered to be known quantities.
- The input to the system is persistently exciting. It is this condition which is necessary and sufficient to ensure asymptotic convergence of parameters.

Application and Simulation Setup

The application in the proposed work is vehicle stability control with differential braking and AFS. Figure 3 shows the block diagram of the simulation setup. The objective of the proposed strategy is to stabilize vehicle motion by control of yaw rate. The vehicle model used in simulations is that contained within the software known as IPG CarMaker. The IPG CarMaker software is used to simulate vehicle dynamics. The multibody vehicle model comprises of a rigid vehicle body taking into account the mass distribution between the carriers, the wheels and the body. Vehicle parameters correspond to a sport utility vehicle and the vehicle model is validated by field tests [53]. The brake and steering models are user-defined and are described in following subsections. The tire dynamics is modeled using Delft-Tire 6.2 with a Magic Formula steady-state slip model describing nonlinear slip forces and moments. The relaxation behaviour is linear using empirical relations for the relaxation lengths.

It is to be noted that in this study, all vehicle state measurements are assumed to be available and noise-free. Furthermore, the vehicle motion is investigated on a flat road devoid of external disturbances such as lateral winds, friction coefficient variations, etc.

Reference Generator

The reference generator provides the desired vehicle yaw rate $\dot{\psi}_{\text{ref}}$. The reference yaw rate is computed using a linear bicycle model:

$$\dot{x}=Ax+B_\delta\delta$$
$$x=\begin{bmatrix} v_y & \dot{\psi}\end{bmatrix}^T$$
$$A=\begin{bmatrix} \frac{-(C_{\alpha f}+C_{\alpha r})}{mv_x} & \frac{-L_fC_{\alpha f}+L_rC_{\alpha r}}{mv_x}-v_x \\ \frac{-L_fC_{\alpha f}+L_rC_{\alpha r}}{I_zv_x} & \frac{-(L_f^2C_{\alpha f}+L_r^2C_{\alpha r})}{I_zv_x}\end{bmatrix} \quad \text{Eq. (23)}$$
$$B_\delta=\begin{bmatrix}\frac{C_{\alpha f}}{m} & \frac{L_fC_{\alpha f}}{I_z}\end{bmatrix}^T$$

FIGURE 3 Proposed control strategy.

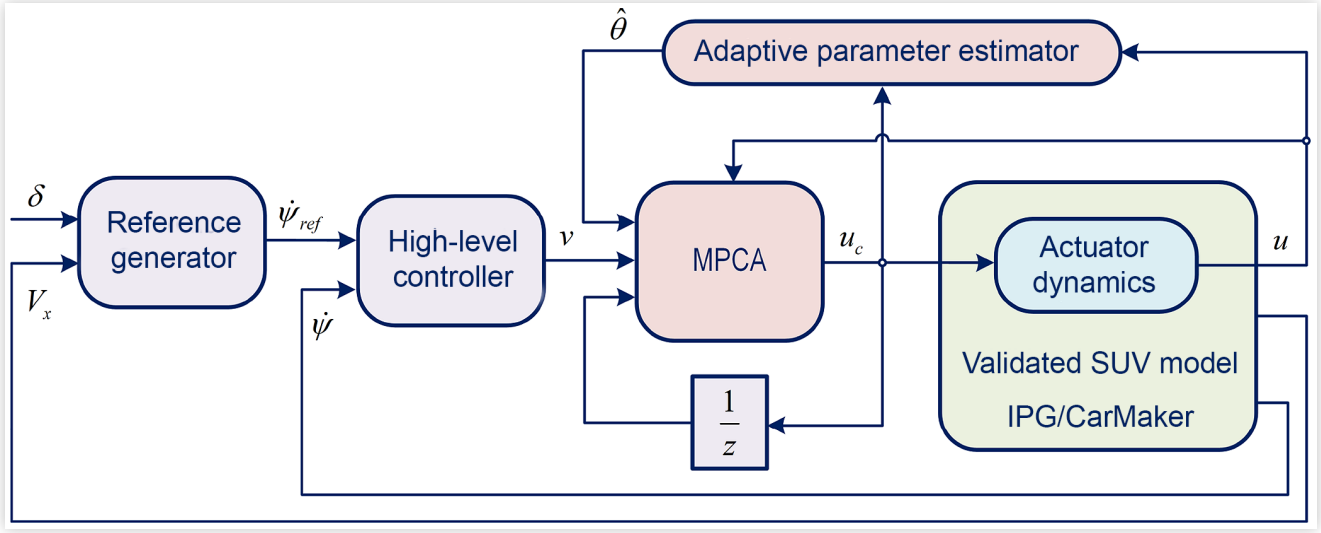

where $C_{\alpha f}$ and $C_{\alpha r}$ are the front and rear axle cornering stiffness. The matrix A is constantly updated with the vehicle longitudinal speed v_x. Other mentioned vehicle parameters and their values are summarized in the Appendix.

The steady-state response of the bicycle model can be written as follows:

$$x_{ss} = \begin{bmatrix} v_{yss} & \dot{\psi}_{ss} \end{bmatrix}^T = -A^{-1} B_\delta \delta \qquad \text{Eq. (24)}$$

As tire saturation is not considered in a linear bicycle model, the peak reference yaw rate computed by the linear bicycle model does not account for the limitations of the road conditions. Therefore, the upper and lower bounds of the yaw rate are

$$\dot{\psi}_{bound} = \left| \frac{\mu g}{v_x} \right| \qquad \text{Eq. (25)}$$

where μ is the friction coefficient and v_x is the longitudinal velocity of the vehicle. The constrained desired yaw rate is then filtered through a second-order transfer function to represent dynamic vehicle response. The natural frequency and damping ratio of this second-order filter is ω_n = 15 rad/sec and ζ = 0.7.

Control Effectiveness Matrix

Also denoted as B is derived using the planar vehicle model combined with the single corner model. The number of actuators considered is 5 as the vehicle is actuated using a combination of differential braking and AFS. In the proposed paper, only yaw rate control is considered. In other words, $v = M_z$ and $u = \begin{bmatrix} T_{bfl} & T_{bfr} & T_{brl} & T_{brr} & \delta_{AFS} \end{bmatrix}^T$. Therefore, the control effectiveness matrix B is defined as follows:

$$B = \begin{bmatrix} \frac{T_f}{2r_w} & -\frac{T_f}{2r_w} & \frac{T_r}{2r_w} & -\frac{T_r}{2r_w} & C_{af} L_f \end{bmatrix} \qquad \text{Eq. (26)}$$

High-Level Controller

The selected high-level controller is a standard discrete-time proportional-derivative regulator operating at 100 Hz:

$$C(z) = K_p + K_d \frac{N}{1 + \frac{NT_s}{z-1}} \qquad \text{Eq. (27)}$$

The corrective yaw moment computed by this controller is denoted by $M_{z,corr}$. The gains are chosen as K_p = 9000, K_d = 1000, N = 1, and T_s = 0.01s. Hence, the virtual control input vector is

$$v(k) = M_{z,\text{corr}}(k) \qquad \text{Eq. (28)}$$

Actuator Dynamics

The simulations carried out employed the use of five actuators such as frictional brakes and steering. It is assumed that each actuator dynamics is a linear one. For the brake system dynamics, the relation between the input pressure to the brake system and the actual calliper pressure is captured using a first-order transfer function model. This model is of the form presented in [54]:

$$\frac{P_{\text{actual}}(s)}{P_{\text{commanded}}(s)} = \frac{1}{\tau s + 1} e^{-\delta_t s} \qquad \text{Eq. (29)}$$

The brake pressure can be converted into a brake torque using a linear relationship $T_{\text{brake}} = P_{\text{P2M}} P_{\text{actual}}$. Brake hysteresis was omitted due to a small influence on the brake performance for a new hydraulic disk brake mechanism [55].

The steering dynamics is simplified and represented by a second-order transfer function with time delay. This dynamic system is of the form [56]:

$$\frac{\delta_{\text{actual}}(s)}{\delta_{\text{commanded}}(s)} = \frac{\omega_n^2}{s^2 + 2\zeta\omega_n s + \omega_n^2} e^{-\delta_t s} \qquad \text{Eq. (30)}$$

MPCA+APE Tuning Parameters

The tuning parameters for the overall CA subsystem are summarized in the Appendix. The weight matrices W and Q need to be resized according to the prediction and control horizons. Lower sampling time of a model predictive control allocator enables it to effectively reject unknown disturbances. On the contrary, a low sampling time for the CA also increases the computational load. In the simulation reported, the selected scenarios are devoid of unknown disturbances, so the sampling time is taken to be the same as that of the high-level controller.

The prediction horizon was chosen in the way that it can look ahead throughout the transient response of the slowest actuator. The control horizon should ideally be kept as low as possible. This is because the number of variables for the optimization problem reduces, thus promoting faster computations and convergence. However, small values of control horizon do not enable the system to respond in the desired way. The control horizon was increased up to a point where the response of the actuator meets the command computed by the MPCA solver.

A general block diagram where APE is combined with MPCA is shown in Figure 3. It is to be noted that the APE requires knowledge of the order of the system, the delay, and the input and output of the dynamics to be estimated. The estimated parameters are then fed back into the MPCA algorithm following which the CA problem is solved with the knowledge of the estimated actuator dynamics.

Results and Discussions

The standard ISO Sine with Dwell (SWD) test was chosen to evaluate the proposed system. The initial vehicle speed was 80 km/h and the amplitude of the steering wheel angle was chosen as 130°. The simulation results obtained using the APE+MPCA method were compared with the WLS CA technique. The WLS technique is a quadratic-programming-based CA method, which does not account for actuator dynamics [23]. To have a proper comparison between two methods, the settings of the high-level control are kept constant.

As can be observed in Figure 4, the vehicle performs the manouevre at friction limits. For the APE+MPCA method, the control system is able to stabilize a vehicle. This is in contrast with the WLS technique failing to ensure stable vehicle motion. The WLS usage results in a significantly higher loss of speed and more than 0.5 g of lateral acceleration even after the steering input has ended and the lateral and yaw motion persists even after the maneuver has ended. The actuator commands for both methods are shown in Figure 5. As WLS does not consider actuator dynamics, the response of the actuator does not meet the required command. As a result, the control fails to pass the manouevre.

It can be seen from Figures 4 and 5 that the WLS method is incapable of optimally coordinating different actuators when slower actuator dynamics are present. This is in contrast with the APE+MPCA technique ensuring effective actuator coordination. Therefore, the WLS technique is applicable only under the assumption of a quick actuator response.

Figures 6 and 7 show the objective assessment of vehicle performance within a SWD test using the quantitative criteria. These criteria are (i) the lateral displacement at 1.07 s after the beginning of steering action must be greater than 1.83 m, and (ii) yaw rate after 1 and 1.75 s after completion of steering action must not exceed 20% and 35% of the peak yaw rate, respectively. In the simulations reported, the steering action begins at 10 s. According to the criteria described in [57], red and green dashed lines have been added in Figures 6 and 7. If the yaw response lies within the green line band, the maneuver is successful. Passage through the red lines indicates failure. From Figure 7, it can be clearly seen that the control system is initially in action till about 12 s, following which the tracking error increases significantly.

The results show the upside of accounting for actuator dynamics in the CA problem. To evaluate the benefit of the APE algorithm, the convergence of actuator parameters is assessed. Figure 8 shows the convergence of the brake actuator parameters. The converged parameters represent the coefficients of the corresponding discrete-time transfer function (in Z-domain) of the brake dynamics. As the response of the actuators are fit into a input-delayed first-order discrete-time dynamic system, the parameters $p(1)$ and $p(2)$ are as follows:

$$y(k+1) = p(1)\,y(k) + p(2)\,u(k-1) \qquad \text{Eq. (31)}$$

The difference Equation 31 can be converted into a linear-in-the-parameters model as described in Equation 21. It can be seen that the parameters converge almost

FIGURE 4 Vehicle response—WLS-CA and APE+MPCA.

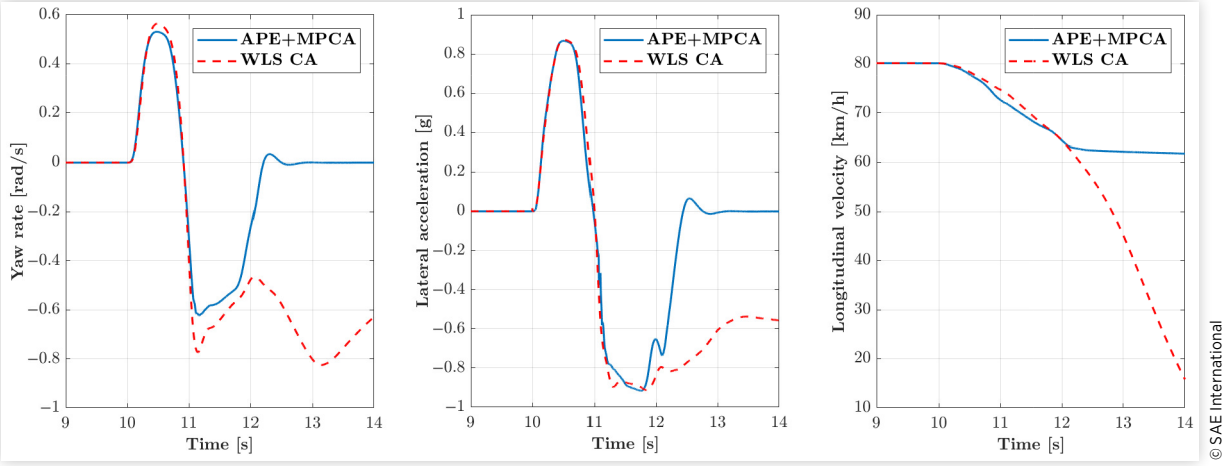

FIGURE 5 Actuator response—WLS-CA and APE+MPCA.

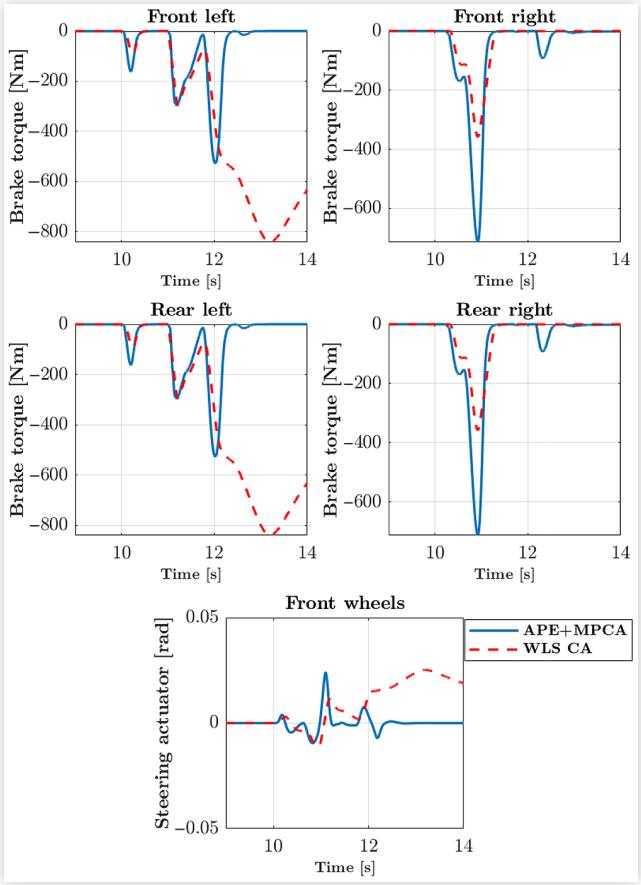

FIGURE 6 Yaw rate response—WLS-CA.

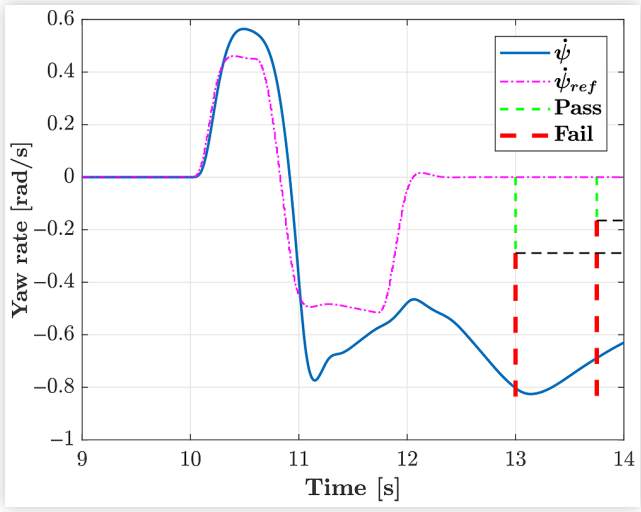

FIGURE 7 Yaw rate response—APE+MPCA.

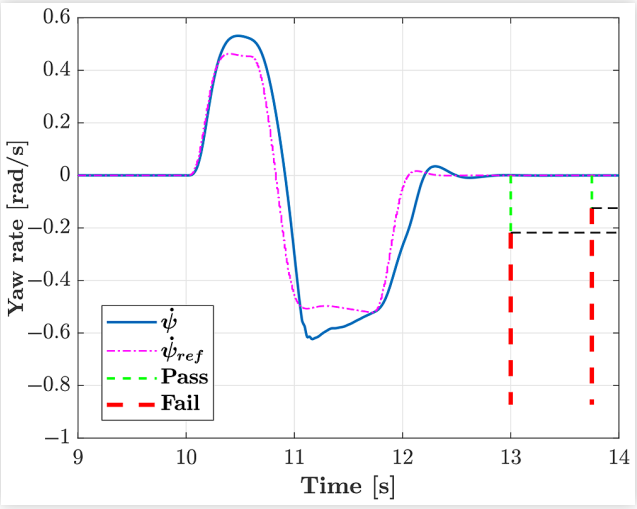

immediately when the maneuver begins. The MPCA solver was initialized with the incorrect set of the actuator parameters and the APE effectively compensates it. A similar evaluation has been done for the steering actuator. The response of the steering actuator, although governed by second order dynamics, it fits into a reduced first order approximation. As it has been shown in the previous section, the steering dynamics maps the driver input to the road wheel angle. Figure 9 compares the road wheel angle estimated by the APE and that calculated in IPG CarMaker. The results indicate that the reduced order approximation using the APE method is reasonable.

Conclusions and Scope for Future Work

This work aims at the effective coordination of actuators for integrated vehicle motion control. It has been shown that the MPCA method combined with an online parameter estimator fulfils this requirement. Accounting for actuator dynamics has been a challenge in the study of CA and MPCA helps in overcoming this issue. During the vehicle operation cycle, the actual actuator dynamics parameters could vary significantly. This issue can be effectively solved by online parameter estimator.

In this study, the actuator dynamics were linear. To capture more details of actuator behavior, linear models become inadequate. The precise models of actuators can help to achieve more accurate coordination between vehicle subsystems. A

FIGURE 8 Brake actuator parameters convergence.

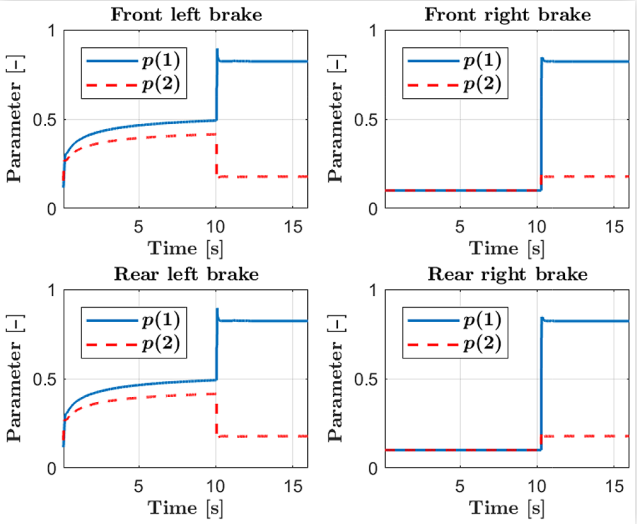

natural consequence of accounting for nonlinear actuator dynamics would be the application of nonlinear MPCA. Furthermore, the online parameter estimator also relies on the assumption that the actuator dynamics are linear in nature and that the order, number of zeros and delay of the system is known. By accounting for nonlinear actuator dynamic descriptions, the approach used to estimate its parameters would need to be re-evaluated as the AM-RLS estimation technique would not be adequate. Considering all these points, there exist a definite potential for improvement by incorporating these considerations in future.

FIGURE 9 Road wheel angle—APE+MPCA.

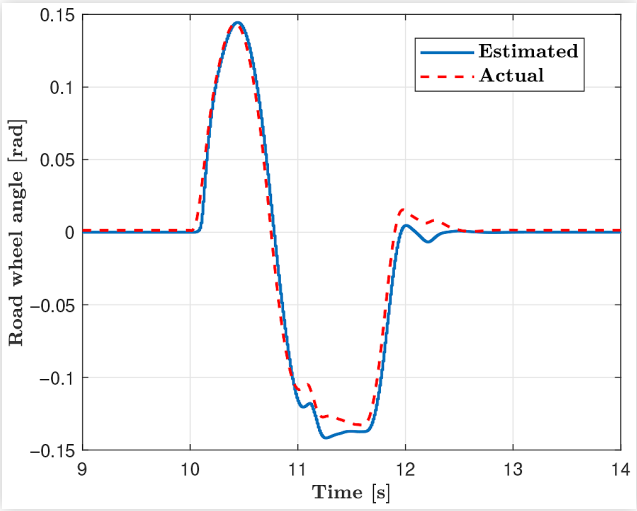

References

1. Reif, K., *Brakes, Brake Control and Driver Assistance Systems* (Weisbaden, Germany: Springer Vieweg, 2014).
2. Johansen, T.A. and Fossen, T.I., "Control Allocation - A Survey," *Automatica* 49(5):1087-1103, 2013.
3. Durham, W., Bordignon, K.A., and Beck, R., *Aircraft Control Allocation* (Chichester: John Wiley & Sons, 2017).
4. Bodson, M., "Evaluation of Optimization Methods for Control Allocation," *Journal of Guidance, Control, and Dynamics* 25(4):703-711, 2002.
5. Schiebahn, M., Zegelaar, P.W., Lakehal-Ayat, M., and Hofmann, O., "The Yaw Torque Influence of Active Systems and Smart Actuators for Coordinated Vehicle Dynamics Controls," *Vehicle System Dynamics* 48(11):1269-1284, 2010.
6. Orend, R., "Modelling and Control of a Vehicle with Single-Wheel Chassis Actuators," *IFAC Proceedings Volumes* 38(1):79-84, 2005.
7. Feiqiang, L., Jun, W., and Zhaodu, L., "On the Vehicle Stability Control for Electric Vehicle Based on Control Allocation," in in *IEEE Vehicle Power and Propulsion Conference*, Harbin, China, 1-6, 2008.
8. Weiskircher, T. and Müller, S., "Control Performance of a Road Vehicle with Four Independent Single-Wheel Electric Motors And Steer-by-Wire System," *Vehicle System Dynamics* 50(sup1):53-69, 2012.
9. Feng, C., Ding, N., He, Y., Xu, G. et al., "A Control Allocation Algorithm for Improving the Fail-Safe Performance of an Electric Vehicle Brake System," *SAE Int. J. Passeng. Cars - Electron. Electric. Syst.s* 6(1):134-143, 2013, https://doi.org/10.4271/2013-01-0187.
10. Shyrokau, B. and Wang, D., "Coordination of Steer Angles, Tyre Inflation Pressure, Brake and Drive Torques for Vehicle Dynamics Control," *SAE Int. J. Passeng. Cars - Mech. Syst.* 6(1):241-251, 2013, https://doi.org/10.4271/2013-01-0712.
11. Plumlee, J.H., Bevly, D.M., and Hodel, A.S., "Control Allocation in Ground Vehicles," *International Journal of Vehicle Design* 42(3-4):215-243, 2006.
12. Knobel, C., Pruckner, A., and Bünte, T., "Optimized Force Allocation - A General Approach to Control and to Investigate the Motion of Over-Actuated Vehicles," in *IFAC Symposium on Mechatronic Systems*, Heidelberg, Germany, 2006.
13. Schofield, B. and Hagglund, T., "Optimal Control Allocation in Vehicle Dynamics Control for Rollover Mitigation," in *American Control Conference*, Seattle, WA, 3231-3236, 2008.
14. Laine, L. and Fredriksson, J., "Traction and Braking of Hybrid Electric Vehicles Using Control Allocation," *International Journal of Vehicle Design* 48(3-4):271-298, 2008.
15. Omerdic, E. and Roberts, G., "Thruster Control Allocation for Over-Actuated, Open-Frame Underwater Vehicles," *IEE Control Engineering Series* 69:87, 2006.

16. Wang, J. and Longoria, R.G., "Coordinated and Reconfigurable Vehicle Dynamics Control," *IEEE Transactions on Control Systems Technology* 17(3):723-732, 2009.
17. Gerard, M. and Verhaegen, M., "Global and Local Chassis Control Based on Load Sensing," in *American Control Conference*, St. Louis, MO, 677-682, IEEE, 2009.
18. Viehweider, A., Salvucci, V., Hori, Y., and Koseki, T., "Improving EV Lateral Dynamics Control Using Infinity Norm Approach with Closed-Form Solution," in *IEEE International Conference on Mechatronics*, Vicenza, Italy, 388-393, 2013.
19. Khosravani, S., Jalali, M., Khajepour, A., Kasaiezadeh, A. et al., "Application of Lexicographic Optimization Method to Integrated Vehicle Control Systems," *IEEE Transactions on Industrial Electronics* 65(12):9677-9686, 2018.
20. Tjonnas, J. and Johansen, T.A., "Stabilization of Automotive Vehicles Using Active Steering and Adaptive Brake Control Allocation," *IEEE Transactions on Control Systems Technology* 18(3):545-558, 2009.
21. Tavasoli, A. and Naraghi, M., "Comparison of Static and Dynamic Control Allocation Techniques for Integrated Vehicle Control," *IFAC Proceedings Volumes* 44(1):7180-7186, 2011.
22. Arat, M.A., Singh, K., and Taheri, S., "Optimal Tire Force Allocation by Means of Smart Tire Technology," *SAE Int. J. Passeng. Cars - Mech. Syst.* 6(1):163-176, 2013, https://doi.org/10.4271/2013-01-0694.
23. Härkegård, O., "Backstepping and Control Allocation with Applications to Flight Control," Ph.D. thesis, Linköpings Universitet, Linköping, 2003.
24. Yildiz, Y., Kolmanovsky, I.V., and Acosta, D., "A Control Allocation System for Automatic Detection and Compensation of Phase Shift due to Actuator Rate Limiting," in *American Control Conference*, San Francisco, CA, 444-449, 2011.
25. Bächle, T., Graichen, K., Buchholz, M., and Dietmayer, K., "Model Predictive Control Allocation in Electric Vehicle Drive Trains," *IFAC-PapersOnLine* 48(15):335-340, 2015.
26. Satzger, C., de Castro, R., and Bünte, T., "A Model Predictive Control Allocation Approach to Hybrid Braking of Electric Vehicles," in *IEEE Intelligent Vehicles Symposium Proceedings*, Dearborn, MI, 286-292, 2014.
27. Zhao, H., Ren, B., Chen, H., and Deng, W., "Model Predictive Control Allocation for Stability Improvement of Four-Wheel Drive Electric Vehicles in Critical Driving Condition," *IET Control Theory & Applications* 9(18):2688-2696, 2015.
28. Jing, H., Jia, F., and Liu, Z., "Multi-Objective Optimal Control Allocation for an Over-Actuated Electric Vehicle," *IEEE Access* 6:4824-4833, 2018.
29. Zhuo, G., Wu, C., and Zhang, F., "Model Predictive Control for Feasible Region of Active Collision Avoidance," SAE Technical Paper 2017-01-0045, 2017, https://doi.org/10.4271/2017-01-0045.
30. Baumann, M., Buchholz, M., and Dietmayer, K., "A Two-Wheel Driven Power Train for Improved Safety and Efficiency in Electric Motorbikes," *World Electric Vehicle Journal* 8(1):102-111, 2016.
31. Sinigaglia, A., Tagesson, K., Falcone, P., and Jacobson, B., "Coordination of Motion Actuators in Heavy Vehicles Using Model Predictive Control Allocation," in *IEEE Intelligent Vehicles Symposium*, Athens, Greece, 590-596, 2016.
32. Kissai, M., Monsuez, B., Mouton, X., Martinez, D. et al., "Model Predictive Control Allocation of Systems with Different Dynamics," in *IEEE Intelligent Transportation Systems Conference*, Auckland, New Zealand, 4170-4177, 2019.
33. Davidson, J.B., Lallman, F.J., and Bundick, W.T., "Integrated Reconfigurable Control Allocation," in *AIAA Guidance, Navigation, and Control Conference and Exhibit*, Montreal, Canada, 1-11, 2001.
34. Xiong, L. and Yu, Z., "Control Allocation of Vehicle Dynamics Control for a 4 In-Wheel-Motored EV," in *IEEE Conference on Power Electronics and Intelligent Transportation System*, Shenzhen, China, vol. 2, 307-311, 2009.
35. Chen, Y. and Wang, J., "An Adaptive Energy-Efficient Control Allocation on Planar Motion Control of Electric Ground Vehicles," in *IEEE Conference on Decision and Control and European Control Conference*, Orlando, FL, 8062-8067, 2011.
36. Pennycott, A., De Novellis, L., Gruber, P., Sorniotti, A. et al., "Enhancing the Energy Efficiency of Fully Electric Vehicles via the Minimization of Motor Power Losses," in *IEEE International Conference on Systems, Man, and Cybernetics*, Manchester, 4167-4172, 2013.
37. Xiong, L., Yu, Z., Wang, Y., Yang, C. et al., "Vehicle Dynamics Control of Four In-Wheel Motor Drive Electric Vehicle Using Gain Scheduling Based on Tyre Cornering Stiffness Estimation," *Vehicle System Dynamics* 50(6):831-846, 2012.
38. Wang, R. and Wang, J., "Fault-Tolerant Control with Active Fault Diagnosis for Four-Wheel Independently Driven Electric Ground Vehicles," *IEEE Transactions on Vehicular Technology* 60(9):4276-4287, 2011.
39. Zong, C., Liu, C., Zheng, H., and Liu, J., "Fault Tolerant Control against Actuator Failures of 4WID/4WIS Electric Vehicles," SAE Technical Paper 2013-01-0405, 2013, https://doi.org/10.4271/2013-01-0405.
40. Kang, J. and Heo, H., "Control Allocation Based Optimal Torque Vectoring For 4WD Electric Vehicle," SAE Technical Paper 2012-01-0246, 2012, https://doi.org/10.4271/2012-01-0246.
41. Brembeck, J. and Ritzer, P., "Energy Optimal Control of an over Actuated Robotic Electric Vehicle Using Enhanced Control Allocation Approaches," in *IEEE Intelligent Vehicles Symposium*, Madrid, Spain, 322-327, 2012.
42. De Novellis, L., Sorniotti, A., and Gruber, P., "Optimal Wheel Torque Distribution for a Four-Wheel-Drive Fully

Electric Vehicle," *SAE Int. J. Passeng. Cars - Mech. Syst.* 6(1):128-136, 2013, https://doi.org/10.4271/2013-01-0673.

43. Bayar, K., Wang, J., and Rizzoni, G., "Development of a Vehicle Stability Control Strategy for a Hybrid Electric Vehicle Equipped with Axle Motors," *IMechE Part D: J. Automobile Engineering* 226(6):795-814, 2012.
44. Shyrokau, B., Wang, D., Savitski, D., Hoepping, K. et al., "Vehicle Motion Control with Subsystem Prioritization," *Mechatronics* 30:297-315, 2015.
45. Zhao, Y., Deng, W., Wu, J., and He, R., "Torque Control Allocation Based on Constrained Optimization with Regenerative Braking for Electric Vehicles," *International Journal of Automotive Technology* 18(4):685-698, 2017.
46. Chen, Y. and Wang, J., "Design and Experimental Evaluations on Energy Efficient Control Allocation Methods for Overactuated Electric Vehicles: Longitudinal Motion Case," *IEEE/ASME Transactions on Mechatronics* 19(2):538-548, 2013.
47. Lee, J., Choi, J., Yi, K., Shin, M. et al., "Lane-Keeping Assistance Control Algorithm Using Differential Braking to Prevent Unintended Lane Departures," *Control Engineering Practice* 23:1-13, 2014.
48. Sundqvist, B.-g., "Vehicle Control System and Method Using Control Allocation and Phase Compensation," U.S. Patent 9,008,939, Apr. 14 2015.
49. Ghoneim, Y.A., Chen, S.-K., Pylypchuk, V., Moshchuk, N.K. et al., "Real-Time Allocation of Actuator Torque in a Vehicle," U.S. Patent 8,655,528, 2014.
50. Wang, L., *Model Predictive Control System Design and Implementation Using MATLAB®* (London: Springer Science & Business Media, 2009).
51. Ding, F., Liu, P.X., and Liu, G., "Gradient Based and Least-Squares Based Iterative Identification Methods for OE and OEMA Systems," *Digital Signal Processing* 20(3):664-677, 2010.
52. Liu, Y., Xie, L., and Ding, F., "An Auxiliary Model Based on a Recursive Least-Squares Parameter Estimation Algorithm for Non-Uniformly Sampled Multirate Systems," *IMechE Part I: Journal of Systems and Control Engineering* 223(4):445-454, 2009.
53. Savitski, D., Ivanov, V., Shyrokau, B., Pütz, T. et al., "Experimental Investigations on Continuous Regenerative Anti-Lock Braking System of Full Electric Vehicle," *International Journal. of Automotive Technology* 17(2):327-338, 2016.
54. Zhou, J., Lu, J., and Peng, H., "Vehicle Stabilization in Response to Exogenous Impulsive Disturbances to the Vehicle Body," in *American Control Conference*, St. Louis, MO, 701-706, 2009.
55. Shyrokau, B., Wang, D., Augsburg, K., and Ivanov, V., "Vehicle Dynamics with Brake Hysteresis," *IMechE Part D: Journal of Automobile Engineering* 227(2):139-150, 2013.
56. Lu, Z., Shyrokau, B., Boulkroune, B., Van Aalst, S. et al., "Performance Benchmark of State-of-the-Art Lateral Path-Following Controllers," in *IEEE Workshop on Advanced Motion Control*, Tokyo, Japan, 541-546, 2018.
57. Picot, N., Miller, B., Rizzo, M.D., and Klingler, T.A., "FMVSS126 Electronic Stability Control Sine with Dwell Incomplete Vehicle Type 2 Analysis," *SAE Int. J. Passeng. Cars - Mechan. Syst.* 4(1):713-721, 2011, https://doi.org/10.4271/2011-01-0956.

Appendix

TABLE A.1 Vehicle parameters.

Parameter	Value
Total mass, m	1963 kg
Front axle to COG, lf	1.0935 m
Rear axle to COG, lr	1.569 m
Front track width, t_f	1.616 m
Rear track width, t_r	1.613 m
Height of COG, h_{cg}	0.673 m
Effective wheel radius, r_w	0.3706 m
Friction coefficient, μ	1
Front cornering stiffness, $C_{\alpha f}$	149,000 N/rad
Rear cornering stiffness, $C_{\alpha r}$	167,000 N/rad
Vehicle inertia about z-axis, I_{zz}	3386.0 kg·m^2
Steering ratio, s_{ratio}	16

TABLE A.2 APE+MPCA tuning parameters.

Parameter	Value
Weight matrix, W	diag[0;0;1]
Weight matrix, Q	diag([0.1;0.1;0.1;0.1;10^8])
Prediction horizon, N_p	30
Control horizon, N_c	25
Sampling time	10^{-2} s
APE parameter, $P(0)$	$10I_2$
APE parameter, $\hat{\theta}(0)$	[0.1 ; 0.1]

TABLE A.3 Brake actuator parameters.

Parameter	Value
Time constant τ	1/20
Input delay δ_t	0.01 s
Conversion factor PP_2M	11.25
Max. pressure	160 bar
Pressure buildup rate	12, 000/P_{P2M} bar/s
Pressure release rate	8000/P_{P2M} bar/s

TABLE A.4 Steering actuator dynamics parameters.

Parameter	Value
Natural frequency, ω_n	30 rad/s
Damping, ζ	0.7
Input delay, δ_t	0.007 s
Position absolute limit	30°
Rate absolute limit	50 ° /s